Coded Aperture Design for Compressive X-ray Tomosynthesis via Coherence Analysis

A. Parada-Mayorga,
University of Delaware
Email: alejopm@udel.edu,

A. Cuadros,
University of Delaware
Email: cuadrosa@udel.edu,

G. R. Arce,
University of Delaware
Email: arce@udel.edu

***Abstract*—The design of coded apertures for compressive X-ray tomosynthesis is addressed here, based on the analysis of the coherence of the sensing matrix. It is shown that minimizing the inner products between the columns of the transfer function matrix, it is possible to obtain significant improvements with respect to the results obtained with the use of random codes. The computational cost of optimization is dramatically lower than other approaches introduced recently.**

I. Introduction

X-ray tomosynthesis imaging plays an important role in biomedical imaging applications like mammography and angiography [3]. As in most X-ray computational tomography imaging systems, radiation exposure can significantly increase the risk of adverse radiation effects, producing damages in body cells [11]. To reduce the damage that radiation can cause, different approaches have been proposed by lowering the number of angles at which projections are taken [12]. However, the consequent reduction of measurements leads to an ill-posed problem, highly sensitive to modeling and measurement errors. Moreover, the reconstructions based on filtered backprojection (FBP) with ill-posed systems of equations produces artifacts and noise which makes the reconstructions useless for medical diagnosis [9][7].

In order to acquire measurements in parallel, coded aperture X-ray tomosynthesis was introduced in [1]. The substantial differentiation in this approach is the use of a coded aperture between the sources of radiation and the objects. This coded aperture codes the radiation signal that impinges on the object allowing a differentiation between the projections on the detector. As a consequence, multiple projections can be captured at the same time instead of capturing sequential measurements as it is done in conventional systems [1]. The projections used in [1], however, used totally random coded apertures. No coded aperture optimization was considered. The optimized design of coded apertures for the compressive X-ray tomosynthesis system was considered first in [2], the results obtained in [2] were superior to the ones obtained with totally random patterns. However, the computational complexity required for the computation of the optimized codes in [2] is high and the objective function used for that purpose is only indirectly linked with the parameters

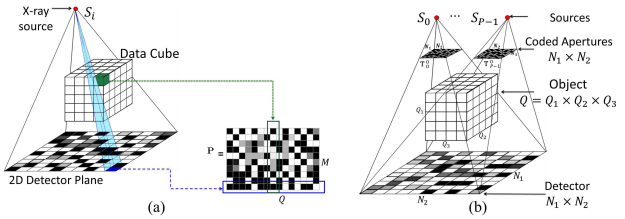

Fig. 1: (a)The matrix $\mathbf{P}$ determines the mapping of the X-ray sources to the detector. (b) Coded aperture compressive X-ray tomosynthesis. The radiation of each source is modulated by the coded aperture.

that are commonly used in compressed sensing. In this work, the coded aperture design is addressed considering the analysis of the coherence of the sensing matrix. It exploits the highly structured sensing matrix that represents the X-ray tomosynthesis architecture. The idea is to minimize the inner products between columns of the sensing matrix considering a general basis representation of the signal of interest. It is shown that, families of codes can be obtained which provide better results than the ones obtained by the use of totally random patterns, and the results can be also comparable to the ones obtained in [2]. The reduction in the computation of the solution is dramatic, because the solution is obtained in seconds whereas in [2] the time is in the order of hours.

This paper is organized as follows. In Section II, the forward model of the computed tomography problem is presented. In the Section III the analysis of the coherence of the sensing matrix is considered adapting the methods presented in [10], an analytical solution for the coded apertures is derived. In Section IV a set of simulations are computed in order to show the performance of the designs obtained with the approach presented in this work in comparison with the totally random patterns and the designs presented in [2]. In Section VI the conclusions of this work are presented.

II. Forward Projection Model

Lets consider an X-ray source that is located at position $\vec{s}$ and radiates an object in direction $\widehat{\theta}$, the continuous X-ray model is given by: $y(\vec{s},\widehat{\theta}) = \int_0^\infty f(\vec{s} + x\widehat{\theta})dx$, where the function f corresponds to the three-dimensional object of

978-1-5090-1172-8/17/$31.00 ©2017 IEEE

Authorized licensed use limited to: University of Pennsylvania. Downloaded on December 13,2020 at 21:16:35 UTC from IEEE Xplore. Restrictions apply.

interest. This imaging model is known as the X-ray transform [2][12].

Because only a discrete number of radon measurements can be acquired, the continuous model is discretized. Let $\mathbf{F} \in \mathbb{R}^{Q_1 \times Q_2 \times Q_3}$ be the three dimensional array that represents the object. The value of Q_1 indicates the number of slices of dimensions $Q_2 \times Q_3$. The detector considered is of dimension $N_1 \times N_2$ and is placed under the considered object as indicated in Fig 1(a).

The projection measurements are represented by the vector $\mathbf{y}$. Then, the traditional forward model in tomosynthesis can be written as $\mathbf{y} = \mathbf{P}\vec{\mathbf{F}}$ where $\vec{\mathbf{F}}$ is a vectorized version of $\mathbf{F}$, and the matrix $\mathbf{P}$ is the system matrix obtained by specifying the hardware settings. The entries of $\mathbf{P}$ correspond to the mapping of the cone-beam energy radiating from the X-ray source onto the detector [2]. As it is shown in Fig. 1(a), each entry of $\mathbf{P}$ represents the portion of the volume of a given voxel that is irradiated by the X-ray associated with one detector element. In particular, each row of $\mathbf{P}$ indicates the information gathered by one detector and each column corresponds to the information gathered from a single voxel [2].

In compressive X-ray tomosynthesis the measurements are multiplexed from multiple sources onto the detector. Coded apertures are located between the sources and the object to modulate the radiation of each source producing a coded projection onto the detector plane [1]. The size of the elements of the coded apertures is fixed to obtain a one to one correspondence with the detector elements [2]. Let $\mathbf{T}_i^{(k)}$ be the coded aperture related with the source i in the shot k, then the measurements $\mathbf{y}$ can be represented as

$$\mathbf{y} = \mathbf{C}\mathbf{P}\vec{\mathbf{F}} \tag{1}$$

where the matrix $\mathbf{C}$ is given by

$$\mathbf{C} = \begin{bmatrix} \mathbf{C}_1^{(1)} & \mathbf{C}_2^{(1)} & \dots \mathbf{C}_S^{(1)} \\ \mathbf{C}_1^{(2)} & \mathbf{C}_2^{(2)} & \dots \mathbf{C}_S^{(2)} \\ & \vdots & \\ \mathbf{C}_1^{(K)} & \mathbf{C}_2^{(K)} & \dots \mathbf{C}_S^{(K)} \end{bmatrix} \tag{2}$$

where $\mathbf{C}_i^{(k)} = \text{diag}\left(\mathbf{T}_i^{(k)}\right)$. The problem (1) is ill conditioned and cannot be solved using traditional approaches. Compressed sensing allows the solution of this problem considering an sparse representation of $\vec{\mathbf{F}}$ in one basis $\mathbf{\Psi}$. The quality of the reconstructed solution is directly related with the coherence of the matrix $\mathbf{C}\mathbf{P}\mathbf{\Psi}$ [8][4].

Lets consider the representation of $\vec{\mathbf{F}}$ in the basis $\mathbf{\Psi}$ as $\vec{\mathbf{F}} = \mathbf{\Psi}\mathbf{f}$, where $\mathbf{f}$ is the sparse coefficients vector representation. Then, the problem (1) can be equivalently written as $\mathbf{y} = \mathbf{A}\mathbf{f}$ where $\mathbf{A} = \mathbf{C}\mathbf{P}\mathbf{\Psi}$ is the sensing matrix. The solution of this problem via compressed sensing can be obtained as the solution of

$$\hat{\mathbf{f}} = \min_{\mathbf{f}} \frac{1}{2} \|\mathbf{y} - \mathbf{A}\mathbf{f}\|_2^2 + \tau \|\mathbf{f}\|_1 \tag{3}$$

where τ is a regularization parameter.

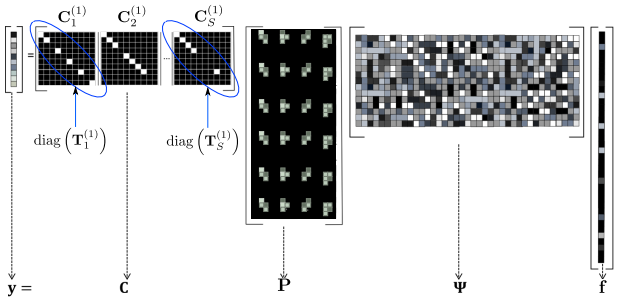

Fig. 2: A graphical representation of the sensing matrix is depicted when $K = 1$ shots and S sources are considered. The matrix $\mathbf{C}$ is composed by the diagonalized version of the coded apertures related to each source.

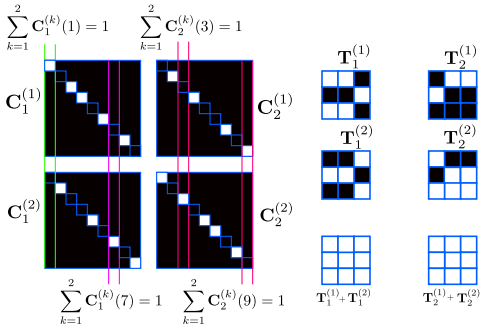

Fig. 3: A graphical representation of the matrix $\mathbf{C}$ is depicted, showing the effects of the condition $\sum_{k=1}^{K} \mathbf{C}_i^{(k)}(u) = 1$ when the number of shots is $K = 3$ and the number of sources is $S = 2$.

III. Analysis of the Sensing Matrix and Coded Aperture Optimization

A measure of the quality of the solutions of (3) in compressed sensing is given by the coherence of the sensing matrix, which is the maximum absolute value for the normalized inner products between any two columns of the sensing matrix [8][4]. The value of this parameter is desired to be as small as possible, to guaranty unique recovery and low error in the numerical solution of the problem as the quality of the solution is directly related to the coherence [5].

In [10] an approach based on the analysis of the coherence was developed to exploit the structure of the sensing matrix in compressive spectral imaging, in order to increase the quality of the reconstructions. The approach proposed in [10] shows how an upper bound of the coherence can be minimized, analyzing the structure of the inner products of the transfer function matrix of the system. It is shown, that when the set of measurements is given by $\mathbf{y} = \mathbf{H}\mathbf{\Psi}\mathbf{f}$, it is possible to achieve a minimum for an upper bound of the coherence when the inner products for the columns of the matrix $\mathbf{H}$ are minimized. In this work, this approach is used to consider the computed tomography problem such that a designed sensing matrix is obtained minimizing the inner products in the matrix $\mathbf{H} = \mathbf{C}\mathbf{P}$, considering arbitrary values on the entries of $\mathbf{P}$.

Authorized licensed use limited to: University of Pennsylvania. Downloaded on December 13,2020 at 21:16:35 UTC from IEEE Xplore. Restrictions apply.

The inner product of the columns m and n of the matrix $\mathbf{CP}$ is given by

$$\varphi_{m,n} = \sum_{u=1}^{N^2} \sum_{k=1}^{K} \sum_{i=1}^{S} \sum_{j=1}^{S} \mathbf{C}_i^{(k)}(u) \mathbf{C}_j^{(k)}(u) Q_{u,u}^{(i,j)}(m,n) \quad (4)$$

where $Q_{u,u}^{(i,j)}(m,n) = \mathbf{P}_u^{(i)}(m)\mathbf{P}_u^{(j)}(n)$ with $\mathbf{P}_u^{(i)}(m)$ representing the $m^{th}-$component of the row u of the projection submatrix i related with the source i. Additionally the convention $\mathbf{C}_i^{(k)}(u) \equiv \mathbf{C}_i^{(k)}(u,u)$ is used to simplify the notation.

Equation (4) can be equivalently written as

$$\varphi_{m,n} = \sum_{u=1}^{N^2} \sum_{i=1}^{S} \left(\sum_{k=1}^{K} \mathbf{C}_i^{(k)}(u) \right) Q_{u,u}^{(i,i)}(m,n) + \cdots$$

$$+ \sum_{u=1}^{N^2} \sum_{i \neq j} \left(\sum_{k=1}^{K} \mathbf{C}_i^{(k)}(u) \mathbf{C}_j^{(k)}(u) \right) Q_{u,u}^{(i,j)}(m,n) \quad (5)$$

Taking into account that $Q_{u,u}^{(i,j)}(m,n) \geq 0$, it follows that the minimum of $\varphi_{m,n}$ is achieved when the terms $\sum_{k=1}^{K} \mathbf{C}_i^{(k)}(u)$ and $\sum_{k=1}^{K} \mathbf{C}_i^{(k)}(u)\mathbf{C}_j^{(k)}(u)$ are minimized. Additionally, using the Cauchy-Schwartz inequality the following relation is obtained

$$\sum_{k=1}^{K} \mathbf{C}_i^{(k)}(u) \mathbf{C}_j^{(k)}(u) \leq \sqrt{\sum_{k=1}^{K} \mathbf{C}_i^{(k)}(u)} \sqrt{\sum_{k=1}^{K} \mathbf{C}_j^{(k)}(u)}. \quad (6)$$

From this relation it is possible to see that the minimization of $\sum_{k=1}^{K} \mathbf{C}_i^{(k)}(u)$ and $\sum_{k=1}^{K} \mathbf{C}_i^{(k)}(u)\mathbf{C}_j^{(k)}(u)$ is achieved by the minimization of $\sum_{k=1}^{K} \mathbf{C}_i^{(k)}(u)$. Because the entries of the coded apertures are represented by binary nonnegative entries, this minimization is achieved when[1]

$$\sum_{k=1}^{K} \mathbf{C}_i^{(k)}(u) = 1. \quad (7)$$

Then, the family of solutions for the coded apertures that satisfy this equality can be written as $\left[\mathbf{C}_i^{(1)}(u), \mathbf{C}_i^{(2)}(u), \ldots, \mathbf{C}_i^{(K)}(u)\right]^T = \boldsymbol{\pi}\{\text{diag}(\mathbf{1}_{K\times 1})\}_1 \ \forall u$, where $\boldsymbol{\pi}$ represents the random permutation operator of the columns, and the subindex 1 the first column of the matrix after applying $\boldsymbol{\pi}$.

IV. Simulations

In order to have a precise comparison with the approach presented in [2], the same simulation scenario is considered. Then, to simulate the compressive X-ray tomosynthesis the configuration of a flat 2D detector plane composed by $N_1 \times N_2 = 150 \times 150$ elements, $S = 9$ cone-beam X-ray sources placed uniformly in a 3×3 geometry and an object of interest $\mathbf{F}$ of dimensions $Q_2 \times Q_3 \times Q_1 = 128 \times 128 \times 16$ are used. Each pixel in the coded aperture corresponds to a particular detector element as detailed in Fig. 4(a). Therefore, the coded apertures placed in front of each of the sources are also composed by 150×150 elements.

[1]The zero solution is not considered because using it would imply that there would be a voxel that is not sensed in any of the shots used in the measurement process

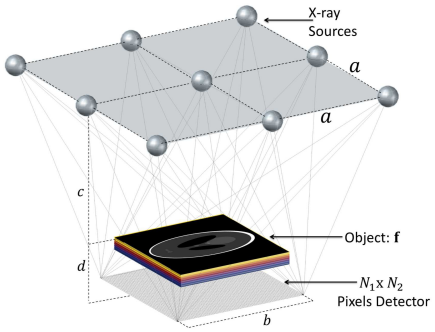

(a)

Fig. 4: (a) Configuration for X-ray tomosynthesis simulation. The 9 sources are placed uniformly over a 128×128 phantom with 16 slices. For the simulation scenario that was studied here $a = 128, b = 128, c = 675, d = 60, e = 150$

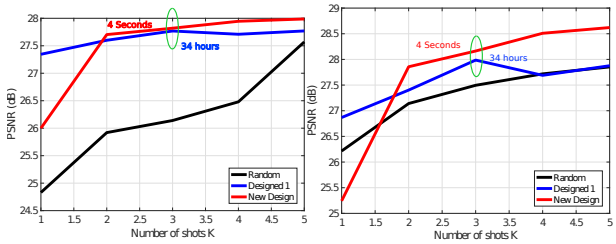

Fig. 5: Left: PSNR of the 13^{th} slice in the reconstructed datacube. Right: The mean PSNR of the reconstructed datacube. $K = 3$ shots are considered. The results obtained in [2] are depicted in blue color whereas the new designs in red color.

The ASTRA Tomography Toolbox (All Scale Tomographic Reconstruction Antwerp) [13] is used to obtain the system matrix $\mathbf{P}$ as well as the projection measurements for each of the X-ray cone beam sources. The codes developed according to the ideas presented in Section III are generated and compared with the totally random codes and the codes generated in [2]. In the last case the algorithm developed in [2] is used to obtain a set of codes for $K = 1, 2, 3, 4, 5$ shots. The GPSR algorithm [6] is used for the reconstructions, doing an experimental tunning of the regularization parameter.

A. Results

Figure 5 plots the PSNR of all the reconstructions obtained. It is possible to appreciate that for a number of shots from $K = 2$ up to $K = 5$ the PSNR of the reconstructions with the designed codes is superior. Also appealing is that the time necessary to generate those codes is in the order of seconds. Figure 5 also shows that the time necessary to obtain the designed codes according to [2] for $K = 3$ shots is 34 hours, whereas the designs obtained with the presented

Authorized licensed use limited to: University of Pennsylvania. Downloaded on December 13,2020 at 21:16:35 UTC from IEEE Xplore. Restrictions apply.

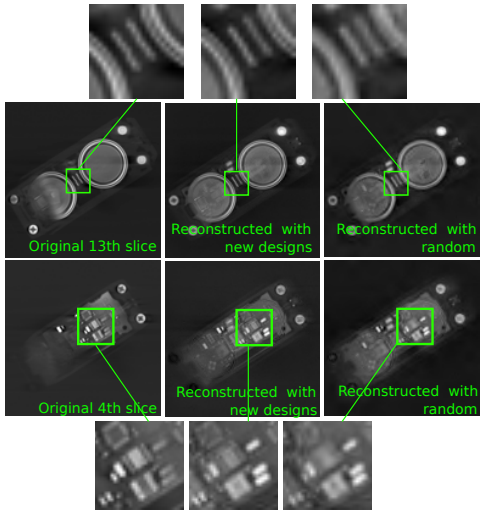

Fig. 6: The slices 4 and 13 of the reconstructed datacube are depicted, comparing the results of using random codes versus the new design approach.

PSNR on 13^{th}-slice			
K	New approach	Approach of [2]	Random
1	**26**	27.34	24.83
2	**27.70**	27.6	25.92
3	**27.82**	27.76	26.14
4	**27.94**	27.70	26.48
5	**27.98**	27.76	27.57
Mean PSNR			
1	**25.24**	26.86	26.21
2	**27.85**	27.40	27.14
3	**28.16**	27.98	27.49
4	**28.50**	27.68	27.71
5	**28.62**	27.87	27.85

TABLE I: The PSNR on the 13^{th} slice is indicated for the different codes used and also the mean PSNR is indicated.

approach is 4 seconds. Additionally in Figure 6 the slices 4^{th} and 13^{th} are showed when random codes are used against the results obtained with the new designs. In the zoomed regions it is clear that with the new designs more details in the reconstructed object can be obtained. In Table I the values of the PSNR obtained in the simulations and used in Fig. 5 are showed. In Figure 7 a sample of the coded apertures obtained by the use of the new approach can be appreciated. Additionally the time spent in the generation of the coded apertures in each approach for different number of shots is presented in Table II for an object of size 32x32x4.

K	1	2	3	4	5
Random	0.21ms	0.3ms	0.22ms	0.23ms	0.39ms
New Design	18.65ms	22.66ms	27.39ms	34.50ms	38.41ms
Designed 1	87.54s	1395s	1411s	3725s	4601s

TABLE II: Time spent in the generation of the coded apertures for each approach and different values of K when the scene considered is of size 32x32x4.

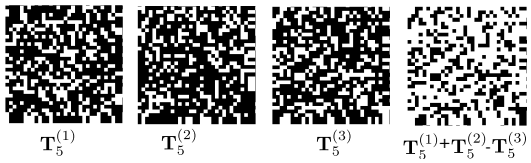

Fig. 7: A 64×64 window of the designed coded aperture with the new design approach is depicted for the source number 5 when $K = 3$ shots are considered.

V. Conclusions

A new strategy for the design of coded apertures in compressed X-ray tomosynthesis has been presented. The proposed approach relies on the analysis of the coherence of the sensing matrix and allows to obtain a family of designs that has a closed form solution. The results of the simulations, show that the designs obtained with the presented approach are better than the results obtained with totally random patterns and with the designs generated in [2]. Additionally, the time necessary to generate the designed codes in the presented approach is in the order of seconds while in [2] is in the order of hours.

References

[1] Kerkil Choi and David J. Brady. Coded aperture computed tomography. *Proc. SPIE*, 7468:74680B–74680B–10, 2009.

[2] Angela P. Cuadros, Christopher Peitsch, Henry Arguello, and Gonzalo R. Arce. Coded aperture optimization for compressive x-ray tomosynthesis. *Opt. Express*, 23(25):32788–32802, Dec 2015.

[3] J. T. Dobbins III and D. J. Godfrey. Digital x-ray tomosynthesis: current state of the art and clinical potential. *Physics in Medicine and Biology*, 48(19):p.R65, 2003.

[4] M. Elad. *Sparse and Redundant Representations: From Theory to Applications in Signal and Image Processing*. Springer Publishing Company, Incorporated, 1st edition, 2010.

[5] Y.C. Eldar. *Sampling Theory: Beyond Bandlimited Systems*. Cambridge University Press, 2015.

[6] M. A. T. Figueiredo, R. D. Nowak, and S. J. Wright. Gradient projection for sparse reconstruction: Application to compressed sensing and other inverse problems. Technical report, IEEE Journal of Selected Topics in Signal Processing, 2007.

[7] V. Kolehmainen M. Lassas K. Hmlinen, A. Kallonen. Sparse tomography. *Computational Methods in Science and Engineering, SIAM*, 35:B644–B665, February 2013.

[8] Y. C. Eldar G. Kutyniok M. A Davenport, M. F. Duarte. Introduction to compressed sensing. In Gitta Kutyniok Yonina C. Eldar, editor, *Compressed Sensing*. Cambridge University Press, 2012.

[9] F. Natterer. *The Mathematics of Computerized Tomography*. Classics in Applied Mathematics. Society for Industrial and Applied Mathematics (SIAM, 3600 Market Street, Floor 6, Philadelphia, PA 19104), 1986.

[10] A. Parada-Mayorga and G. Arce. Colored coded aperture design in compressive spectral imaging via minimum coherence. *IEEE Transactions on Computational Imaging-Special Issue in Earth sciences (Submitted)*, 2016.

[11] R. Marcus R. Smith-Bindman, J. Lipson and et al. Radiation dose associated with common computed tomography examinations and the associated lifetime attributable risk of cancer. *Archives of Internal Medicine*, 169(22):2078–2086, 2009.

[12] I. Reiser and S. Glick. *Tomosynthesis Imaging*. CRC press, 2014.

[13] Wei Xu, Fang Xu, Mel Jones, Bettina Keszthelyi, John Sedat, David Agard, and Klaus Mueller. High-performance iterative electron tomography reconstruction with long-object compensation using graphics processing units (gpus). *Journal of Structural Biology*, 171(2):142 – 153, 2010.

Authorized licensed use limited to: University of Pennsylvania. Downloaded on December 13,2020 at 21:16:35 UTC from IEEE Xplore. Restrictions apply.